Using Stochastic Storm Transposition to Update Rainfall Intensity-Duration-Frequency (IDF) Curves for the Coon Creek and West Fork Kickapoo Watersheds

Daniel Wright, PhD
Zhe Li, PhD
Eric Booth, PhD
University of Wisconsin-Madison, Madison, Wisconsin

Contact: Daniel B. Wright; Address: Room 1269 Engineering Hall, 1415 Engineering Drive, Madison, WI 53706, USA; Phone: 608-262-1978; Email: danielb.wright@wisc.edu

Analysis performed for the United States Department of Agriculture, Natural Resources Conservation Service-Wisconsin

July 20, 2020

Executive Summary

Following the failure of five flood control structures in the Coon Creek and West Fork Kickapoo Watersheds in August 2018, the USDA-Natural Resources Conservation Service (NRCS) is working with an architectural and engineering (A&E) firm to produce a Watershed Project Plan-Environmental Impact Statement (PLAN-EIS) for each watershed. This plan requires new economic analyses (cost-benefit) for replacement of the five structures as well as alternatives that prevent or reduce flood damages. These economic analyses will utilize a hydrologic and hydraulic (H&H) model (to be developed by A&E firm) to calculate flood stages for several design storm events. The rainfall values used as input to the H&H model and associated with these design storm events (e.g., 100-year 24-hour event) are commonly sourced from the National Oceanic and Atmospheric Association (NOAA) Precipitation-Frequency Atlas of the United States. The rainfall intensity-duration-frequency (IDF) estimates from this resource–known as Atlas 14 (Volume 8)–are derived from historical rain gage records that typically span several decades but do not include data more recent than 2012. While Atlas 14 is currently the most reliable and widely used source of IDF estimates in the United States, there are growing concerns about the method's inability to 1) incorporate the most recent heavy rainfall events in a given region and 2) account for a non-stationary, warming climate that is resulting in a higher frequency of heavy rainfall events. This inability to account for a widely-recognized phenomenon has the potential to alienate and frustrate regional stakeholders that are being asked to participate in a watershed planning process that will lead to long-term positive economic outcomes in the region.

The University of Wisconsin-Madison was contracted by the NRCS to employ an alternative method known as Stochastic Storm Transposition (SST) to estimate IDF values that accounts for recent extreme heavy rainfall events. This report provides the results of this analysis, as well as background information on how it was performed. The results show that IDF estimates produced by SST are generally more severe than from Atlas 14 at the 24-hour duration. The same is true at the 6-hour duration for recurrence intervals of 100-years and above, while lower recurrence intervals are similar between SST and Atlas 14. Analysis of radar rainfall hyetographs for major storms in the region shows that the NRCS/SCS Type-II rainfall temporal distribution produces more severe intense rainfall rates than most of these observed storms. Careful H&H analysis, however, is needed to determine how the temporal patterns of these observed storms compare with the Type-II, in terms of the flood peak magnitudes and water surface elevations that they produce.

1. Background and Introduction

Following the failure of five flood control structures in the Coon Creek and West Fork Kickapoo Watersheds in August 2018, the USDA-Natural Resources Conservation Service (NRCS) is working with an architectural and engineering (A&E) firm to produce a Watershed Project Plan-Environmental Impact Statement (PLAN-EIS) for each watershed. This plan requires new economic cost-benefit analyses to evaluate the feasibility of replacement of the five structures as well as evaluation of other alternatives to prevent or reduce flood damages. These economic analyses will utilize a hydrologic and hydraulic (H&H) model (to be developed by A&E firm) to calculate flood stages for several design storm events. The rainfall values used as input to the H&H model and associated with these design storm events (e.g., 100-year, 24-hour rainfall events) are commonly sourced from the National Oceanic and Atmospheric Association (NOAA) Precipitation-Frequency Atlas of the United States. The rainfall intensity-duration-frequency (IDF) estimates from this resource–known as Atlas 14 (Volume 8; Perica et al., 2013)–are derived from historical rain gage records that typically span several decades but do not include data more recent than 2012. While Atlas 14 is currently the most reliable and widely used source of IDF estimates in the United States, there are growing concerns about the method's inability to 1) incorporate the most recent heavy rainfall events in a given region and 2) account for a non-stationary, warming climate that is resulting in a higher frequency of heavy rainfall events (Lopez-Cantu and Samaras, 2018; Wright et al., 2019). This inability to account for a widely-recognized phenomenon has the potential to alienate and frustrate regional stakeholders, who are participating in a watershed planning process that will lead to long-term positive economic outcomes in the region.

The University of Wisconsin-Madison was contracted by the NRCS to employ Stochastic Storm Transposition (SST; Fontaine and Potter, 1989; Wilson and Foufoula-Georgiou, 1990; Wright et al., 2017, 2013) as an alternative method to estimate IDF values that accounts for recent extreme heavy rainfall events. A brief description of SST is provided in Section 2.1, while a more detailed description of the methodology and software is provided in Appendix A. Findings of the SST analysis are provided in Section 2.2, while the data and analysis parameters are described in Appendix B. In addition, using the same radar rainfall data used for the SST analysis, ten major storms from the surrounding region are analyzed in terms of their temporal rainfall patterns. In Section 2.3, these patterns are compared against two commonly-used 24-hour temporal rainfall distribution previously developed by the NRCS. A parallel analysis of 6-hour rainfall patterns is provided in Appendix C. Observed and design 6-hour and 24-hour hyetographs for the 28 August 2018 are provided in Appendix D.

2. Findings

2.1 Overview of Stochastic Storm Transposition

Stochastic Storm Transposition (SST) is an alternative to conventional statistically-based rainfall frequency analysis to derive rainfall intensity-duration-frequency (IDF) relationships (Wright et al., 2020, 2013). SST effectively lengthens the extreme rainfall record through temporal resampling and spatial transposition of observed storms from the surrounding region to create many extreme rainfall scenarios. This approach is distinct from more conventional methods. SST also differs from more commonly-used methods in that it relies on spatially complete "rainfall

fields" (i.e. rainfall maps over multiple time steps), rather than long records of rain gage observations at one or several specific sites. Weather radar is one source of rainfall fields, which, when combined with rain gage-based corrections, can provide accurate, spatially complete depictions of rainfall over large areas (Krajewski et al., 2010; Wright et al., 2014).

Unlike rain gage records, which in some locations date back many decades, radar rainfall records are generally only 1-2 decades in length at the present time. In this study, for example, the period of analysis is 18 years (2002-2019). This is generally considered insufficient for estimating rare rainfall recurrence intervals such as the 100-year storm. However, by considering observed storms from a surrounding region that did not strike the location of interest, but could have done so, it is possible to use SST to derive such rare events from relatively short radar rainfall records. The region used in this analysis is shown in the left panel of Figure 1; it includes Wisconsin as well as parts of Illinois, Iowa, Minnesota, and the upper peninsula of Michigan. Rainfall over the great lakes was not included in the analysis. The location of interest in this analysis was the point 43.60° North, 90.90° West. This point, shown in both the left and right panels of Figure 1, fall roughly in the center of the Coon Creek and West Fork Kickapoo watersheds, which are also shown. Testing showed that IDF results are insensitive to the precise location of this point within the general vicinity of the two watersheds (results not shown).

The results of this SST analysis are shown below in Section 2.2. A more detailed overview of SST methodology and the software used in this analysis are described in more detail in Appendix A. The data and specific analysis parameters used in this analysis are described in Appendix B. It should be noted that these results represent point-scale rainfall estimates, comparable to those provided by rain gages. In addition to the use gage-adjust radar rainfall observations, with an additional correction to account for differences between the "pixel" resolution of the radar (roughly 20 km^2) and the point-scale IDF estimates that are sought in this study.

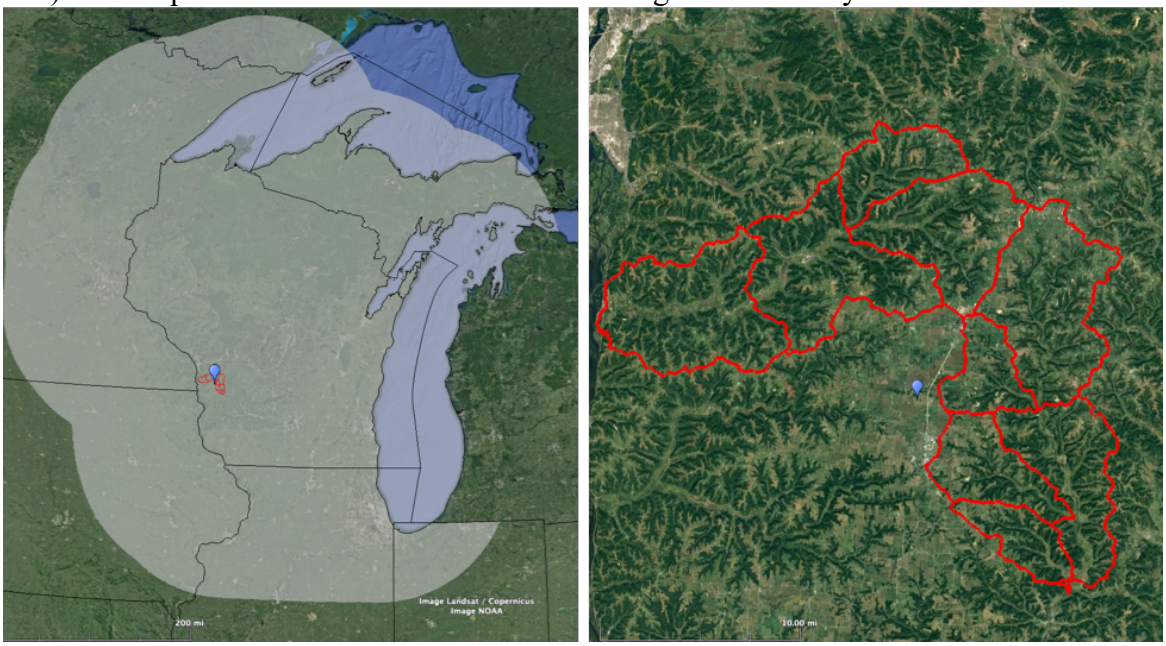

Figure 1: Left: Study region with transposition domain highlighted in lighter shading. Right: study watersheds. In both panels, Coon Creek and West Fork Kickapoo watersheds are shown in red, while blue pin indicates the location for which IDF estimates were produced. While the SST domain is shown as including parts of Lakes Michigan and Superior, rainfall that occurred over the lakes was not considered in the results.

2.2 Intensity-Duration-Frequency (IDF) Results

Tables 1 and 2 show the results of the SST-based 6-hour and 24-hour IDF analyses, respectively. The same data are shown graphically in Figure 2, along with IDF curves of the same duration from Volume 8 of NOAA Atlas 14 (Perica et al., 2013) included for reference. It can be seen from Figure 2 that both the 6-hour and 24-hour SST-based IDF curve lie above the Atlas 14 results for most return periods. At the 24-hour duration, the highest return periods (particularly 1000-year) are relatively similar between SST and Atlas 14.

Table 1: 6-hour duration IDF statistics for point rainfall generated using RainyDay SST software. Atlas 14 statistics for the same location (see Figure 1) are provided.

exceedance probability	Return Period	Atlas 14	lower bound	Mean	upper bound
[-]	[yrs]	[inches]	[inches]	[inches]	[inches]
0.5	2	2.0	2.2	2.2	2.3
0.2	5	2.7	3.0	3.1	3.2
0.1	10	3.3	3.7	3.8	3.9
0.04	25	4.2	4.5	4.8	5.1
0.02	50	4.9	5.1	5.5	5.9
0.01	100	5.7	5.8	6.4	7.0
0.005	200	6.7	6.6	7.5	8.5
0.002	500	8.0	7.3	9.1	11.1
0.001	1000	9.1	8.3	10.6	13.1

Table 2: 24-hour duration IDF statistics generated using RainyDay SST software. Atlas 14 statistics for the same location (see Figure 1) are provided.

exceedance probability	Return Period	Atlas 14	lower bound	Mean	upper bound
[-]	[yrs]	[inches]	[inches]	[inches]	[inches]
0.5	2	2.7	2.8	2.9	3.0
0.2	5	3.5	4.0	4.1	4.2
0.1	10	4.3	4.8	5.0	5.2
0.04	25	5.4	5.8	6.2	6.5
0.02	50	6.5	6.7	7.1	7.6
0.01	100	7.6	7.5	8.2	9.1
0.005	200	8.9	8.4	9.4	10.5
0.002	500	10.8	9.3	11.1	13.0
0.001	1000	12.4	9.8	12.5	14.4

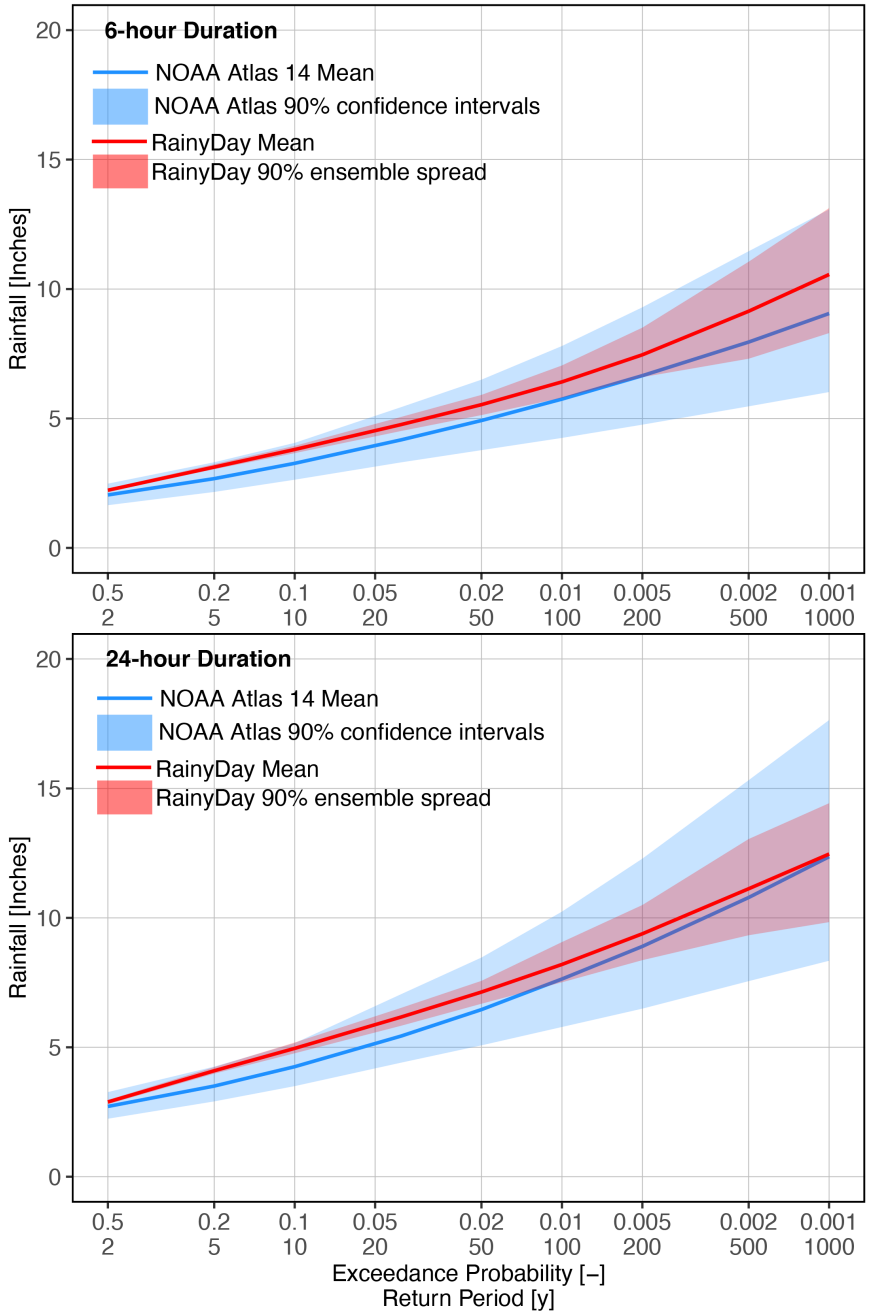

Fig. 2: Top—6-hour IDF curves from Atlas 14 and RainyDay-based SST analysis. Bottom—24-hour IDF curves from Atlas 14 and RainyDay-based SST analysis.

2.3 Rainfall Temporal Analysis

As described in Section 2.1 and Appendices A and B, the SST analysis used radar rainfall-based observations of major storms from the region shown in the left panel of Figure 1. This collection of major storms identified from the radar rainfall data is generally referred to as a "storm catalog" (Wright et al., 2020, 2013). In addition to being useful for generating IDF estimates, these storm catalogs can provide additional insights into the properties of major storms in the region. Of particular interest for flood analyses is the timing, or temporal distribution, of rainfall during storm

events. This timing determines the amount and time of occurrence of maximum streamflow magnitudes and water surface elevations.

Conventional hydrologic engineering practice in the United States often makes use of published temporal distributions provided by the NRCS or other agencies. These temporal distributions can be combined with IDF rainfall depth estimates such as those shown in Figure 2 to distribute those depths over time. In this section, we compare the commonly-used NRCS/SCS Type-II[1] and MSE4[2] 24-hour temporal distributions (which are recommended for use in that west-central Wisconsin) to the temporal distributions of the ten largest storms from the storm catalog used in the SST analysis. It should be noted that the NRCS/SCS distributions were aggregated to the hourly scale from their original shorter timescales. This aggregation is necessary to render it comparable to the hourly-resolution radar rainfall data.

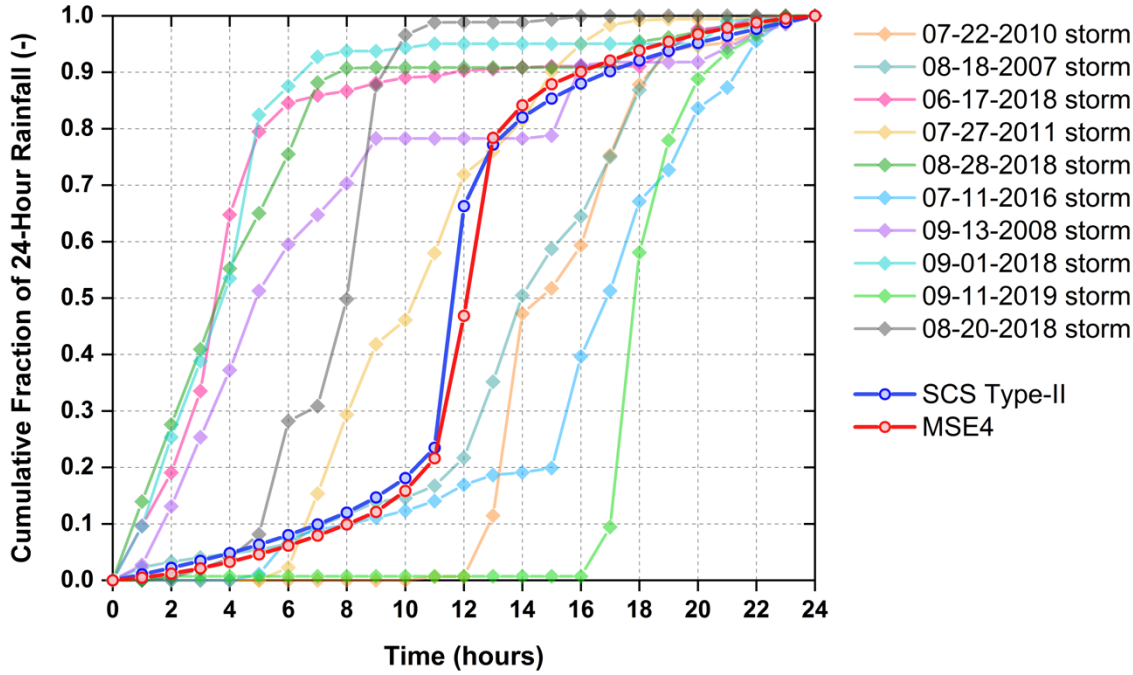

Fig. 3: Comparison of 24-hour dimensionless cumulative time distributions from the ten largest storms from the storm catalog used for the SST analysis. The NRCS/SCS Type-II and MSE4 distributions are also shown.

The cumulative 24-hour time distributions for these ten storms, as well as for the NRCS Type II and MSE4 storms, are shown in Figure 3. The timing of peak rainfall (indicated by the largest "jumps" in Figure 3) vary substantially by storm. This timing can influence flood response. For example, if very high rainfall rates come after a period of lighter rainfall, the flood response can be more severe than if those high rates came before the lighter rainfall, because the soils would be more saturated prior to the onset of heavy rainfall. A parallel analysis for 6-hour rainfall is shown in Appendix C, Figure C1; results are very similar.

Several storms, most notably that of September 11, 2019, had very intense periods of peak rainfall. This storm produced major flood damage near the Wisconsin/Illinois border including in Beloit,

[1] See https://www.nrcs.usda.gov/wps/portal/nrcs/detailfull/national/water/?cid=stelprdb1044959
[2] See National Engineering Handbook Part 650: Peak Discharges Engineering Field Handbook Wisconsin Supplement

WI. The 2019 storm had a peak one-hour jump exceeding that of the NRCS/SCS Type-II storm, while the other nine storms showed peak one-hour jumps somewhat smaller than the NRCS/SCS storm. This means that these other storms had lower rainfall peaks and somewhat more steady rainfall throughout the 24-hour analysis period. These features can be seen more easily in the following Figures 4 through 13, which show the rainfall hyetographs and cumulative hyetographs for the ten storms, which are presented in order from smallest to largest point-scale rainfall accumulation. The NRCS/SCS Type-II storm is also shown. In the left panels of these figures, the total 24-hour rainfall depth used for the Type-II storm is the same as that observed in the storm catalog. Figure 5 in particular highlights the very high peak hourly rainfall for the September 11, 2019 storm.

Compared with the Type II storm, the MSE4 distribution has a somewhat lower peak. Three storms had hourly rainfall peaks exceeding the peak hourly rate of MSE4, while two additional storms had comparable peak hourly rates. Parallel analyses for 6-hour rainfall are shown in Appendix C, Figures C2 to C11. Results at the 6-hour scale confirm the 24-hour scale results.

To summarize, it appears that the NRCS/SCS Type-II temporal distribution yields a more intense peak hourly rainfall rate than all but one of the largest ten storms from the SST analysis, while the MSE4 storm is roughly comparable to the "average" behavior of the ten storms. If used in hydrologic/hydraulic flood simulations, this may mean that the Type-II storm yields larger flood peaks than would be produced using the temporal patterns from those nine storms, while the MSE4 storm may be a more realistic choice. However, additional consideration must be given to the timing of these storms, since the precise sequencing of light and heavy rainfall can influence soil saturation and thus runoff generation and flood response. Previous studies have highlighted the important interaction between increasing heavy rainfall frequency, temporal rainfall distribution, and antecedent moisture conditions (Dullo et al., 2017; Woldemeskel and Sharma, 2016) and this topic is worthy of further investigation in the region.

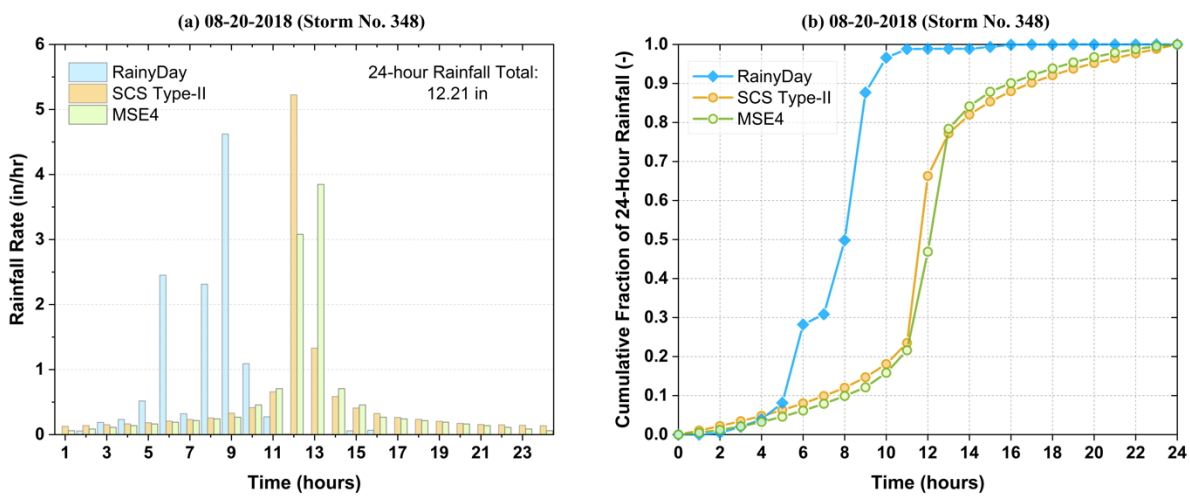

Figure 4: Left—24-hour rainfall hyetograph for the Aug. 20, 2018 storm, and corresponding NRCS/SCS Type-II storm. Right—cumulative rainfall fractions for this storm, with NRCS/SCS Type-II and MSE4 storms provided for comparison.

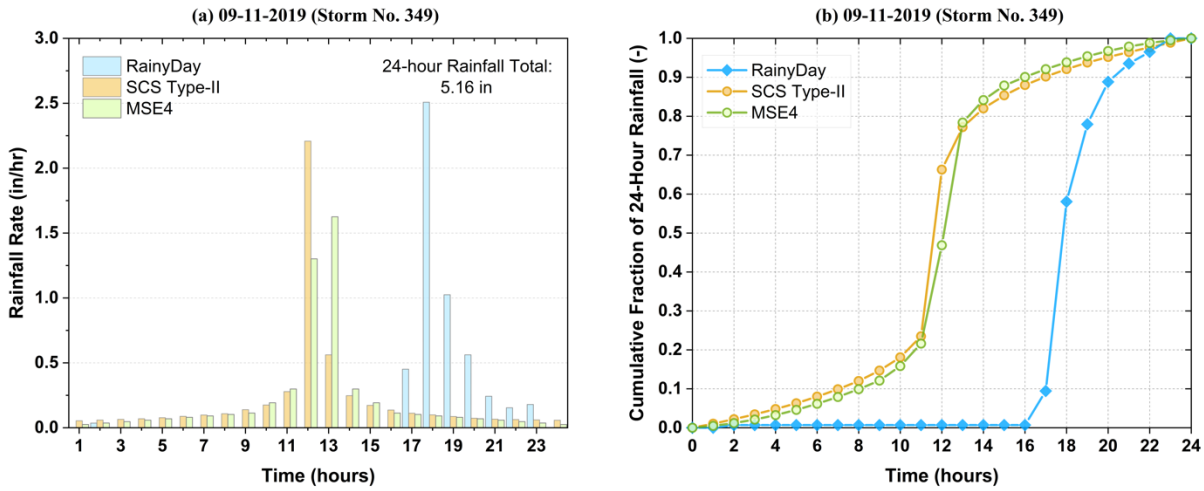

Figure 5: Same as for Figure 4, but for Sep. 9, 2019 storm.

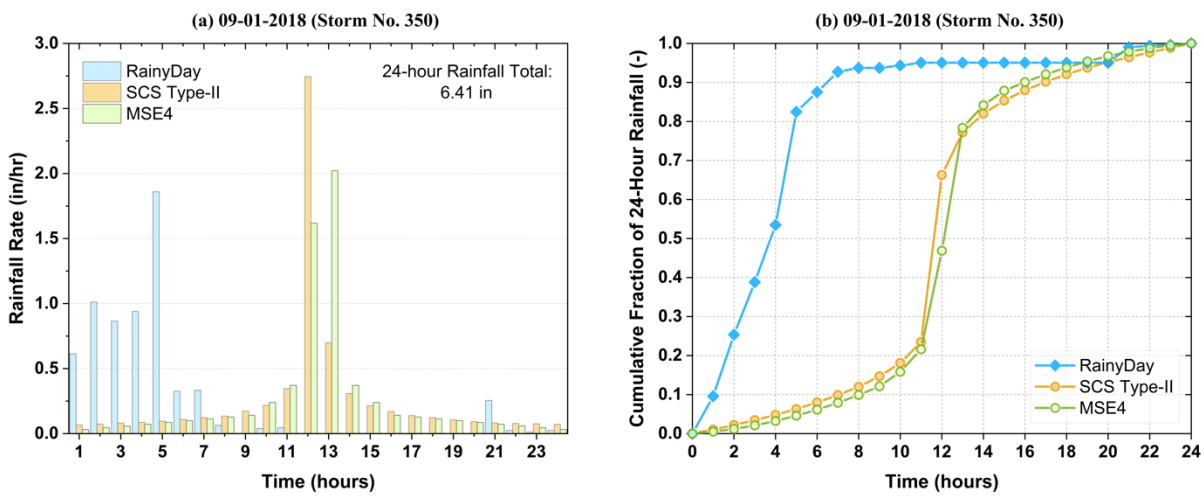

Figure 6: Same as for Figure 4, but for Sep. 1, 2018 storm.

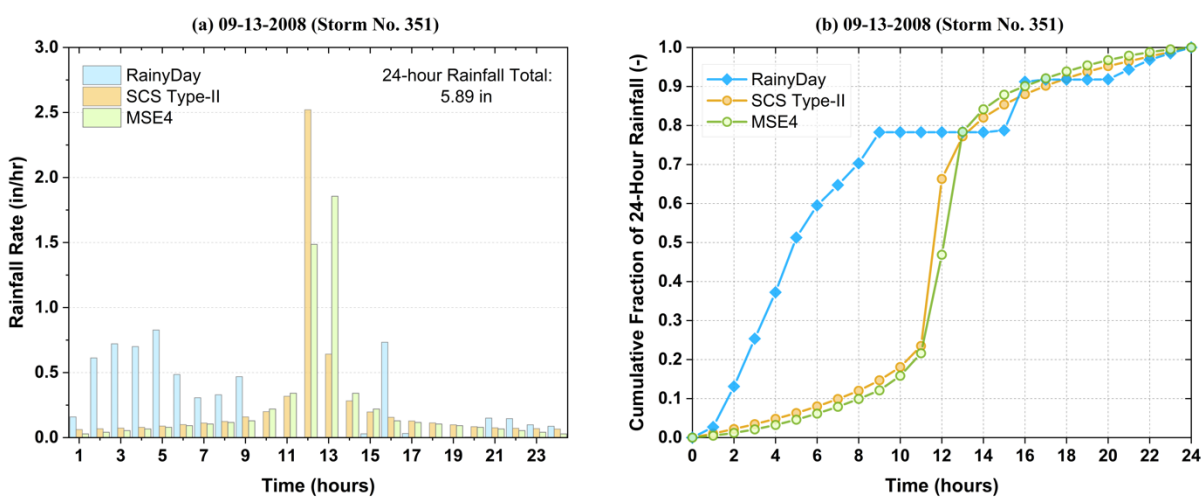

Figure 7: Same as for Figure 4, but for Sep. 13, 2008 storm.

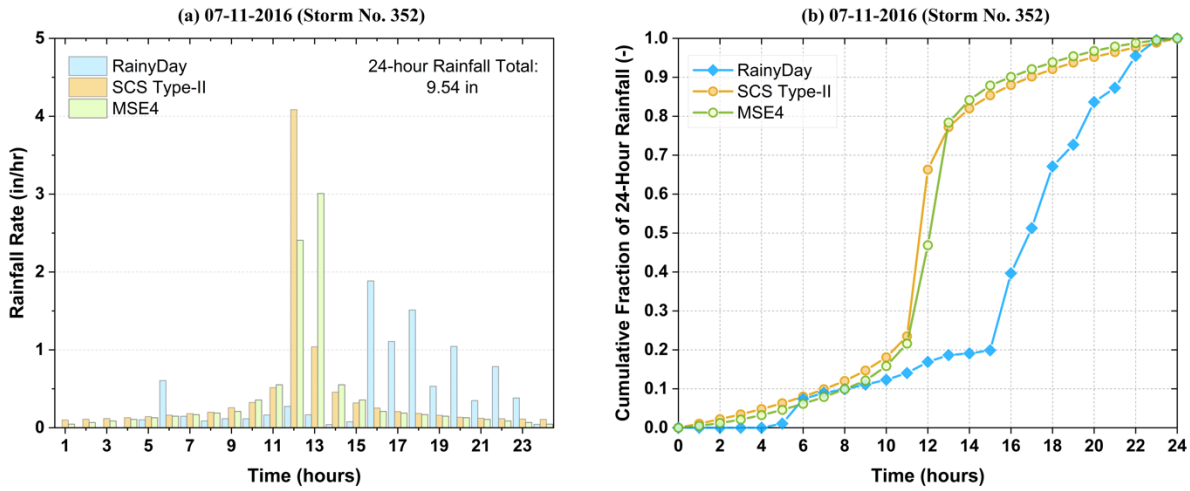

Figure 8: Same as for Figure 4, but for Jul. 11, 2016 storm.

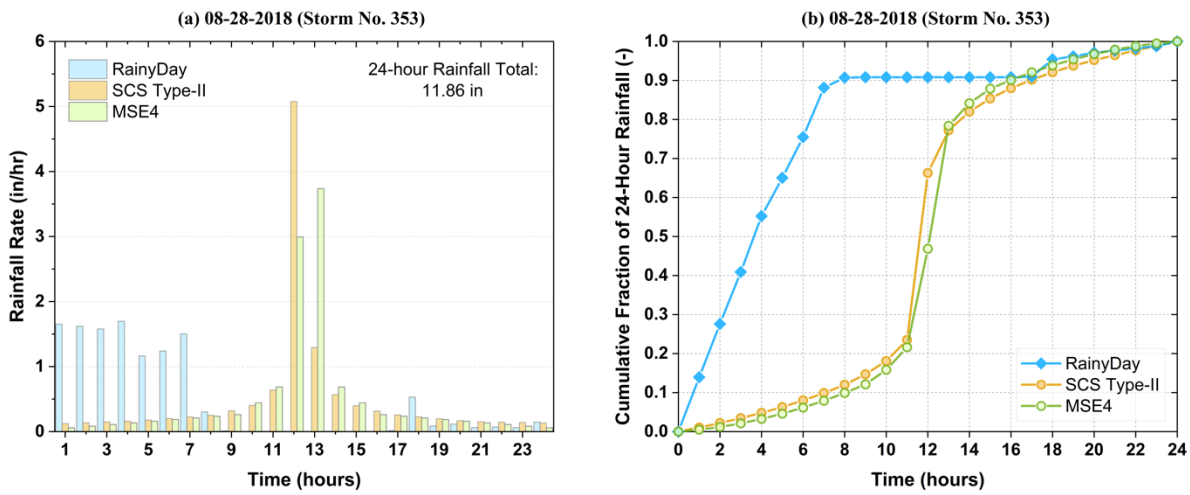

Figure 9: Same as for Figure 4, but for Aug. 28, 2018 storm.

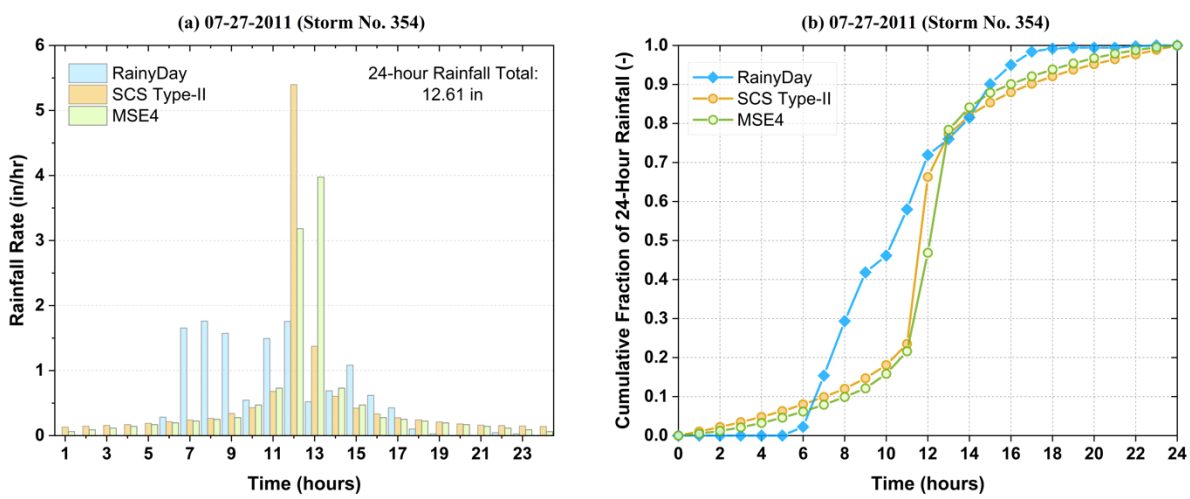

Figure 10: Same as for Figure 4, but for Jul. 27, 2011 storm.

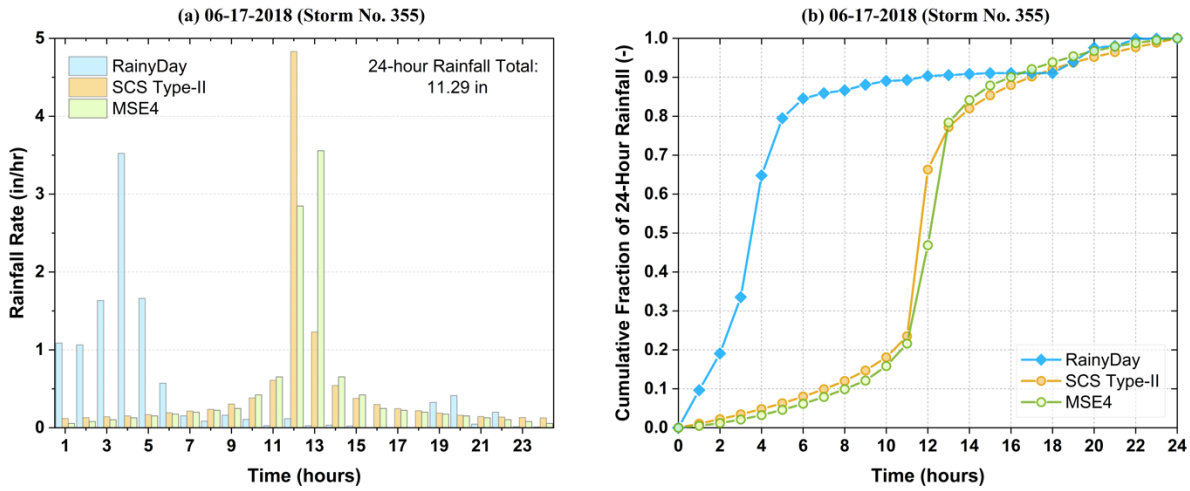

Figure 11: Same as for Figure 4, but for Jun. 17, 2018 storm.

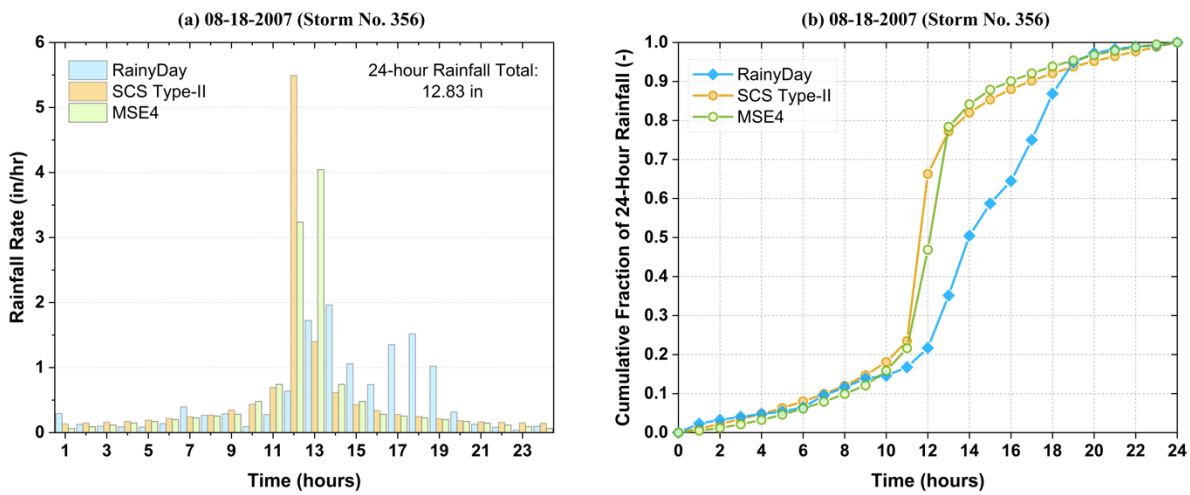

Figure 12: Same as for Figure 4, but for Aug. 18, 2007 storm.

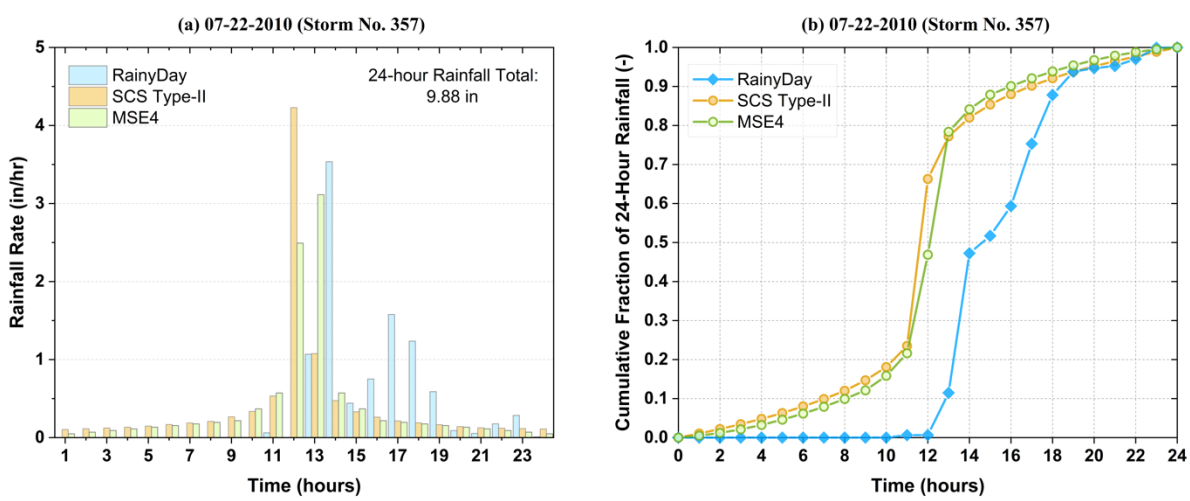

Figure 13: Same as for Figure 4, but for Jul. 22, 2010 storm.

References

Atlas, D., Rosenfeld, D., Short, D.A., 1990. The estimation of convective rainfall by area integrals: 1. The theoretical and empirical basis. J. Geophys. Res. Atmospheres 95, 2153–2160. https://doi.org/10.1029/JD095iD03p02153

Daly, C., Halbleib, M., Smith, J.I., Gibson, W.P., Doggett, M.K., Taylor, G.H., Curtis, J., Pasteris, P.P., 2008. Physiographically sensitive mapping of climatological temperature and precipitation across the conterminous United States. Int. J. Climatol. 28, 2031–2064. https://doi.org/10.1002/joc.1688

Daly, C., Neilson, R.P., Phillips, D.L., 1994. A Statistical-Topographic Model for Mapping Climatological Precipitation over Mountainous Terrain. J. Appl. Meteorol. 33, 140–158. https://doi.org/10.1175/1520-0450(1994)033<0140:ASTMFM>2.0.CO;2

Dullo Tigstu T., Kalyanapu Alfred J., Teegavarapu Ramesh S. V., 2017. Evaluation of Changing Characteristics of Temporal Rainfall Distribution within 24-Hour Duration Storms and Their Influences on Peak Discharges: Case Study of Asheville, North Carolina. J. Hydrol. Eng. 22, 05017022. https://doi.org/10.1061/(ASCE)HE.1943-5584.0001575

England, J.F., Julien, P.Y., Velleux, M.L., 2014. Physically-based extreme flood frequency with stochastic storm transposition and paleoflood data on large watersheds. J. Hydrol. 510, 228–245. https://doi.org/10.1016/j.jhydrol.2013.12.021

Fontaine, T.A., Potter, K.W., 1989. Estimating Probabilities of Extreme Rainfalls. J. Hydraul. Eng. 115, 1562–1575. https://doi.org/10.1061/(ASCE)0733-9429(1989)115:11(1562)

Foufoula-Georgiou, E., 1989. A probabilistic storm transposition approach for estimating exceedance probabilities of extreme precipitation depths. Water Resour. Res. 25, 799–815. https://doi.org/10.1029/WR025i005p00799

Franchini, M., Helmlinger, K.R., Foufoula-Georgiou, E., Todini, E., 1996. Stochastic storm transposition coupled with rainfall—runoff modeling for estimation of exceedance probabilities of design floods. J. Hydrol. 175, 511–532. https://doi.org/10.1016/S0022-1694(96)80022-9

Krajewski, W.F., Villarini, G., Smith, J.A., 2010. Radar-rainfall uncertainties: Where are we after thirty years of effort? Bull. Am. Meteorol. Soc. 91, 87–94. https://doi.org/10.1175/2009BAMS2747.1

Lee, R.-Y., Holland, B.S., Flueck, J.A., 1979. Distribution of a Ratio of Correlated Gamma Random Variables. SIAM J. Appl. Math. 36, 304–320.

Lewis, E., Fowler, H., Alexander, L., Dunn, R., McClean, F., Barbero, R., Guerreiro, S., Li, X.-F., Blenkinsop, S., 2019. GSDR: A Global Sub-Daily Rainfall Dataset. J. Clim. 32, 4715–4729. https://doi.org/10.1175/JCLI-D-18-0143.1

Lin, Y., 2011. GCIP/EOP Surface: Precipitation NCEP/EMC 4KM Gridded Data (GRIB) Stage IV Data. Version 1.0. UCARNCAR - Earth Obs. Lab. https://doi.org/10.5065/D6PG1QDD

Lopez-Cantu, T., Samaras, C., 2018. Temporal and spatial evaluation of stormwater engineering standards reveals risks and priorities across the United States. Environ. Res. Lett. 13, 074006. https://doi.org/10.1088/1748-9326/aac696

Nadarajah, S., 2010. Distribution properties and estimation of the ratio of independent Weibull random variables. AStA Adv. Stat. Anal. 94, 231–246. https://doi.org/10.1007/s10182-010-0134-1

Nadarajah, S., Kotz, S., 2006. ON THE PRODUCT AND RATIO OF GAMMA AND WEIBULL RANDOM VARIABLES. Econom. Theory 22, 338–344. https://doi.org/10.1017/S0266466606060154

Perica, S., Martin, D., Pavlovic, S., Roy, I., St. Laurent, M., Trypaluk, C., Unruh, D., Yekta, M., Bonnin, G.M., 2013. Precipitation-Frequency Atlas of the United States (No. Volume 8 Version 2.0), NOAA Atlas 14. National Oceanic and Atmospheric Administration, Silver Spring, Maryland.

Shimizu, K., 1993. A Bivariate Mixed Lognormal Distribution with an Analysis of Rainfall Data. J. Appl. Meteorol. 32, 161–171. https://doi.org/10.1175/1520-0450(1993)032<0161:ABMLDW>2.0.CO;2

Villarini, G., Krajewski, W.F., 2010. Review of the Different Sources of Uncertainty in Single Polarization Radar-Based Estimates of Rainfall. Surv. Geophys. 31, 107–129. https://doi.org/10.1007/s10712-009-9079-x

Wilson, L.L., Foufoula-Georgiou, E., 1990. Regional Rainfall Frequency Analysis via Stochastic Storm Transposition. J. Hydraul. Eng. 116, 859–880. https://doi.org/10.1061/(ASCE)0733-9429(1990)116:7(859)

Woldemeskel, F., Sharma, A., 2016. Should flood regimes change in a warming climate? The role of antecedent moisture conditions. Geophys. Res. Lett. 43, 7556–7563. https://doi.org/10.1002/2016GL069448

Wright, D.B., Bosma, C.D., Lopez-Cantu, T., 2019. U.S. Hydrologic Design Standards Insufficient Due to Large Increases in Frequency of Rainfall Extremes. Geophys. Res. Lett. 46, 8144–8153. https://doi.org/10.1029/2019GL083235

Wright, D.B., Holman, K.D., 2019. Rescaling Transposed Extreme Rainfall within a Heterogeneous Region. J. Hydrol. Eng. 24, 06019001. https://doi.org/10.1061/(ASCE)HE.1943-5584.0001781

Wright, D.B., Mantilla, R., Peters-Lidard, C.D., 2017. A remote sensing-based tool for assessing rainfall-driven hazards. Environ. Model. Softw. 90, 34–54. https://doi.org/10.1016/j.envsoft.2016.12.006

Wright, Daniel B., Smith, J.A., Baeck, M.L., 2014. Flood frequency analysis using radar rainfall fields and stochastic storm transposition. Water Resour. Res. 50, 1592–1615. https://doi.org/10.1002/2013WR014224

Wright, Daniel B, Smith, J.A., Villarini, G., Baeck, M.L., 2014. Long-Term High-Resolution Radar Rainfall Fields for Urban Hydrology. JAWRA J. Am. Water Resour. Assoc. 50, 713–734. https://doi.org/10.1111/jawr.12139

Wright, D.B., Smith, J.A., Villarini, G., Baeck, M.L., 2013. Estimating the frequency of extreme rainfall using weather radar and stochastic storm transposition. J. Hydrol. 488, 150–165. https://doi.org/10.1016/j.jhydrol.2013.03.003

Wright, D.B., Yu, G., England, J.F., 2020. Six decades of rainfall and flood frequency analysis using stochastic storm transposition: Review, progress, and prospects. J. Hydrol. 585, 124816. https://doi.org/10.1016/j.jhydrol.2020.124816

Yu, G., Wright, D.B., Zhu, Z., Smith, C., Holman, K.D., 2019. Process-based flood frequency analysis in an agricultural watershed exhibiting nonstationary flood seasonality. Hydrol Earth Syst Sci 23, 2225–2243. https://doi.org/10.5194/hess-23-2225-2019

Zhang, L., Singh, V.P., 2007. Bivariate rainfall frequency distributions using Archimedean copulas. J. Hydrol. 332, 93–109. https://doi.org/10.1016/j.jhydrol.2006.06.033

Zhou, Z., Smith, J.A., Wright, D.B., Baeck, M.L., Yang, L., Liu, S., 2019. Storm Catalog-Based Analysis of Rainfall Heterogeneity and Frequency in a Complex Terrain. Water Resour. Res. 55, 1871–1889. https://doi.org/10.1029/2018WR023567

Zhu, Z., Wright, D.B., Yu, G., 2018. The Impact of Rainfall Space-Time Structure in Flood Frequency Analysis. Water Resour. Res. 54, 8983–8998. https://doi.org/10.1029/2018WR023550

Appendix A: SST Methodology

A.1. SST Methodology

The following step-by-step methodology for SST-based rainfall frequency analysis for a user-defined geographic "area of interest," *A* of arbitrary shape is adapted from Wright et al. (2017). *A* can be a single remote sensing pixel, a rectangular area containing multiple pixels, or a contiguous area defined by a user-supplied polygon in shapefile format. Higher-level description of RainyDay software features is left to Appendix A.2.

The following five steps describe the SST methodology, as implemented in the RainyDay software:

1. Identify a geographic transposition domain *A'* that encompasses the area of interest *A*. One could confine *A'* to regions with homogeneous extreme rainfall properties, (e.g. flat areas far from large water bodies and topographic features). However, such homogeneity would likely be difficult to rigorously determine in practice and regardless, such strict interpretation is likely to be overly limiting. RainyDay offers several diagnostic aids that help the user to understand rainfall heterogeneity over the region *A'* and to improve the performance of the SST procedure in cases where rainfall heterogeneities do exist.

2. Identify the largest *m* temporally non-overlapping storms in *A'* from an *n*-year rainfall remote sensing dataset, in terms of rainfall accumulation of duration *t* and with the same size, shape, and orientation of *A*. We refer to this set of storms henceforth as a "storm catalog," with the same geographic extent as *A'* and the same spatial and temporal resolution as the input rainfall data. We refer to the *m* storms in the storm catalog henceforth as "parent storms." In RainyDay, the user can specify whether to exclude certain months (such as wintertime) from the storm catalog. Previous studies have shown that there can be low bias introduced in high-exceedance probability (i.e. frequent, low-intensity) events if *m* is small (Foufoula-Georgiou, 1989; Franchini et al., 1996; Wilson and Foufoula-Georgiou, 1990; Wright et al., 2013). $m \approx 20n$ generally minimizes the low bias for frequent events and would likely be a good starting point for new analyses. Low exceedance probability (i.e. rare) events are insensitive to the choice of *m* (Wright et al., 2017).

   In RainyDay, duration *t* is a user-defined input, and if *t* is neither very short nor very long relative to the time scale of hazard response in *A*, subsequent hazard modeling results will be relatively insensitive to the chosen value. In this respect, the duration *t* in SST differs conceptually from design storm methods, in which hazard response is intrinsically sensitive to the user-specified duration, and this feature is indeed one of the chief advantages of SST over design storm methods for multi-scale flood hazard estimation (Daniel B. Wright et al., 2014). In the case of SST-based flood frequency analysis, *t* should be at least as long as the watershed time of concentration and preferably somewhat longer.

3. Randomly generate an integer *k*, which represents a "number of storms per year." In previous SST literature, the assumption was made that *k* follows a Poisson distribution with a rate parameter λ storms per year. The *m* parent storms are selected such that an average of $\lambda = m/n$ storms per year are included in the storm catalog. For example, if $m = 100$

storms selected from a ten-year remote sensing dataset, then $\lambda = 100/10 = 10.0$ storms per year. RainyDay will generate k using either the Poisson distribution or an empirical distribution derived from storm catalog properties. If the Poisson distribution is selected, RainyDay will automatically calculate λ based on user-specified m and the length of the input dataset.

4. Randomly select k parent storms from the storm catalog. For each selected parent storm, transpose all rainfall fields associated with that storm by an east-west distance Δx and a north-south distance Δy, where Δx and Δy are drawn from the distributions $D_X(x)$ and $D_Y(y)$ which are bounded by the east-west and north-south extents of A', respectively. The motion and structure of the parent storm is unaltered during transposition and only the location is changed. The distributions $D_X(x)$ and $D_Y(y)$ were taken to be uniform in Wright et al. (2013) and (Daniel B. Wright et al., 2014; Wright et al., 2013). RainyDay offers additional options, including a stochastic rescaling option, used in this study and described in Appendix A2.3. We illustrate this step schematically in Figure A1. For each of the k transposed storms, compute the resulting t-hour rainfall accumulation averaged over A.

   Step 4 can be understood as temporal resampling and spatial transposition of observed storm events within a probabilistic framework to synthesize one year of heavy rainfall events over A' and, by extension, over A. RainyDay and previous SST efforts retain the largest (in terms of rainfall intensity) of the k events for subsequent steps and discard the $k-1$ remaining events, though in principle these events could be retained. The single retained storm can be understood as a "synthetic" annual rainfall maximum, analogous to those annual rainfall maxima that are extracted from rain gage records for rainfall frequency analysis. These rainfall events do not form a continuous series, meaning that neither inter-storm periods nor the temporal sequencing of the k storms are considered.

5. Repeat steps 3 and 4 a user-specified T_{max}, number of times, in order to create T_{max} years of t-hour synthetic annual rainfall maxima for A. RainyDay then assigns each annual maxima a rank i according to its rainfall intensity relative to all others. Each of these ranked maxima can then be assigned an annual exceedance probability p_e^i where $p_e^i \equiv i/T_{max}$. Exceedance probability p_e is the probability in a given year that an event of equal or greater intensity will occur. The "return period" or "recurrence interval" T_i, commonly used in hazard analysis, is simply $T_i \equiv 1/p_e^i$, so if $T_{max} = 10^3$, it is possible to directly infer exceedance probabilities of $1.0 \geq p_e \geq 10^{-3}$ (recurrence intervals of $1 \leq T_i \leq 10^3$). Each of these rainfall events can then serve as one datum of an empirical IDF estimate or as a rainfall scenario for hazard modeling.

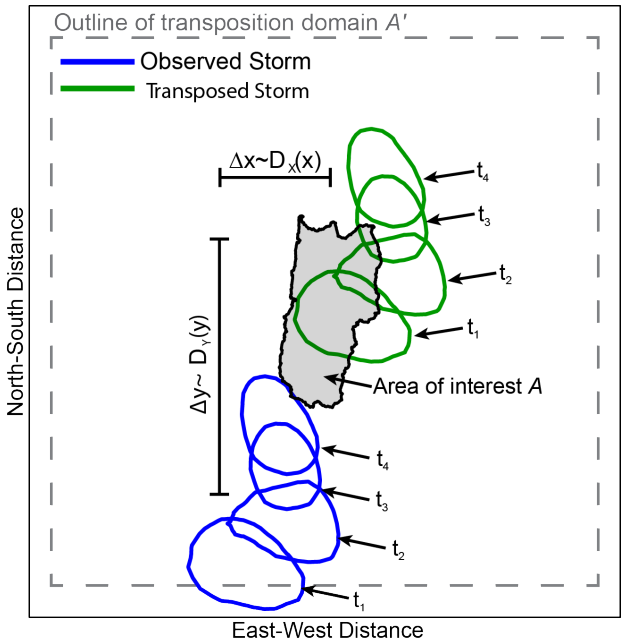

Figure A1: Depiction of SST procedure for a single storm consisting of four time intervals $t_1 ... t_4$. The blue ellipses illustrate the time evolution of an arbitrary rainfall isohyet derived from remote sensing observations, while the green ellipses show the time evolution of the same isohyets after transposition. Adapted from Wright et al. (2013).

A.2 RainyDay Software

A.2.1 Overview of Software

A schematic depiction of the structure of the RainyDay software is shown in Figure A2.

Name of Software: RainyDay Rainfall Hazard Modeling System
Developer: Dr. Daniel B. Wright, PhD
Contact: Daniel B. Wright; Address: Room 1269 Engineering Hall, 1415 Engineering Drive, Madison, WI 53706, USA; Email: danielb.wright@wisc.edu

Required hardware and software: RainyDay requires Python 3.7 or newer (not tested with earlier version of Python 3; not compatible with Python 2).

Access: RainyDay is available free of charge on https://github.com/danielbwright/RainyDay2. It is distributed via the MIT Open Source License: https://opensource.org/licenses/MIT

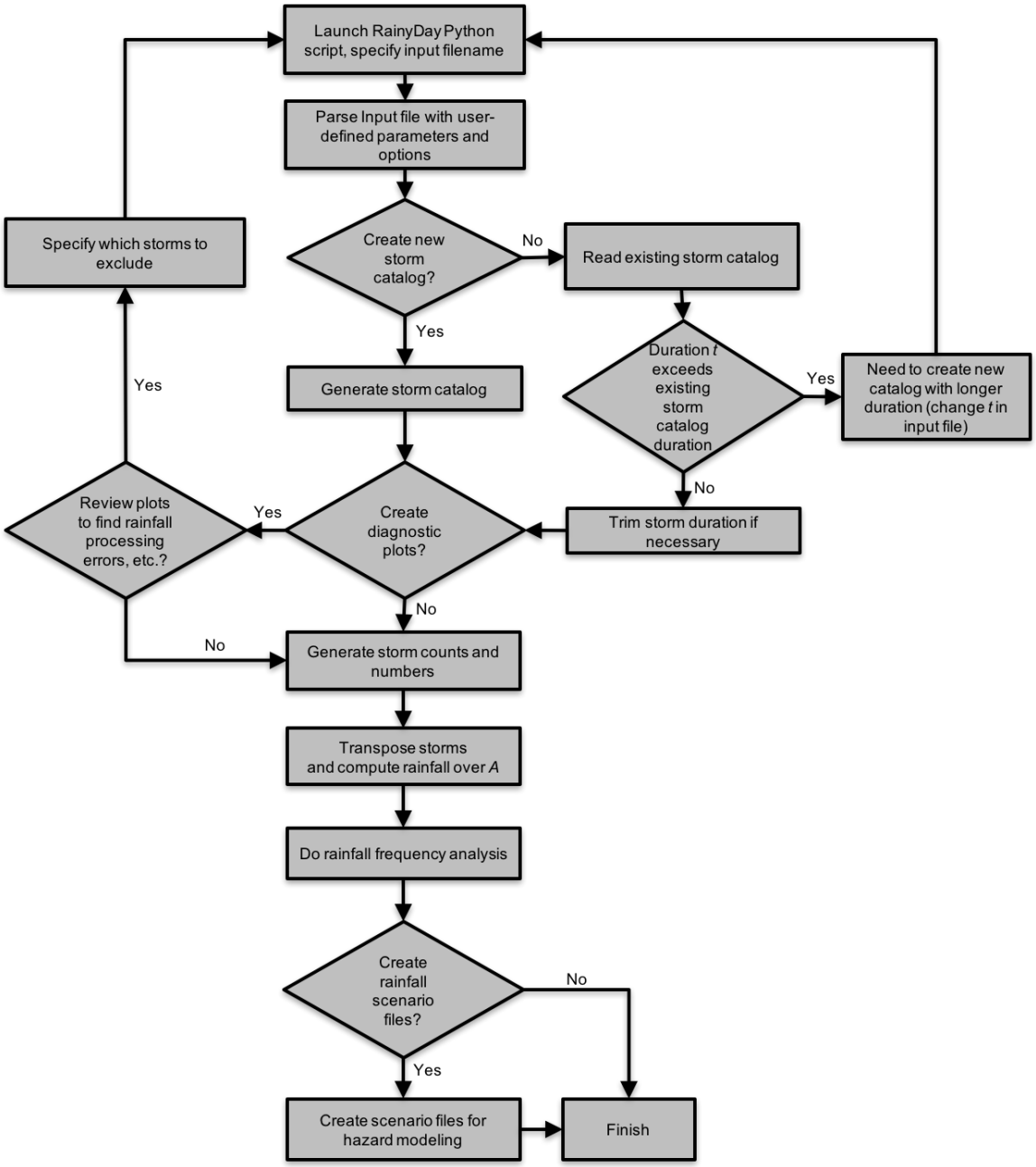

Figure A2: Flow chart demonstrating the workflow of RainyDay.

A.2.2 SST Uncertainty/Confidence Interval Estimation

In RainyDay, the user specifies N, the number of T_{max}-year long "ensemble members" to be generated. This enables examination of "internal variability," i.e. how much variation in rainfall intensity is possible for a given p_e for a given input rainfall dataset and set of user-defined parameters. For example, if the user specifies $T_{max} = 10^3$ and $N = 100$, then there will be 100 intensity estimates for each p_e between 1.0 and 10^{-3}. RainyDay will automatically generate text file and graphics files containing the results of this rainfall frequency analysis, including the rainfall mean, minimum, and maximum (or, optionally, a quantile interval) for each p_e, computed from the N ensemble members. Like virtually all frequency analyses and IDF estimation methods, the

ensemble spread generated by RainyDay does not consider measurement error, which can be substantial. Since the ensemble spread is characteristic to a given set of user-defined values such as *A'* or *m*, it does not consider uncertainty associated with these choices.

A.2.3 Rainfall Heterogeneity and Non-Uniform Spatial Transposition

A common criticism of SST is that its validity is restricted to regions with homogenous extreme rainfall properties. As previously mentioned, depending on how rigidly this criterion is enforced, the method would be limited to small, flat regions far from topographic features, water bodies, etc. It is unclear how homogeneity would be determined, particularly given the paucity of rainfall data in most regions. Instead, steps can be taken to use SST in more varied geophysical settings. Regardless of the setting, the selection of *A'* requires an understanding of regional rainfall patterns and of the intrinsic assumptions of SST. Though more work is needed to understand the geographic limits of the applicability of RainyDay in complex terrain, the work of England et al. (2014) and Zhou et al. (2019) provides an example of SST usage in complex terrain or over heterogeneous domains. Rainfall properties can vary across the transposition domain shown in Figure 1, necessitating the usage of a stochastic "rescaling" procedure for transposed storms. This procedure, described in Wright and Holman (2019), is a stochastic extension of the rainfall multiplier approach introduced in Zhou et al. (2019).

This rescaling approach is based on the concept of a ratio distribution, i.e. the distribution of $R = Y/X$, where X and Y are random variables. Commonly-used ratio distributions include the *F*-distribution (the ratio of two scaled independent Chi-squared distributions) and the Cauchy distribution (the ratio of two independent standard normal distributions). Other ratio distributions have been derived for certain marginals, parameter values, and correlations (e.g. Lee et al., 1979; Nadarajah, 2010; Nadarajah and Kotz, 2006). Few of these are suitable for describing rainfall, and parameter estimation can be challenging. An exception is if both X and Y are lognormally distributed (often a reasonable approximation for rainfall; e.g. Atlas et al., 1990; Shimizu, 1993; Zhang and Singh, 2007), in which case it is straightforward to derive the distribution of R for any parameter set and correlation. Let $X = X_i$ and $Y = X_j$, the lognormally-distributed rainfall at locations i and j with linear correlation $\rho_{X,Y}$. Thus:

$$logR = log\left(\frac{Y}{X}\right) = logY - logX.$$

By definition, $logX$ and $logY$ are normally distributed with parameters $\{\mu_X, \sigma_X^2\}$ and $\{\mu_Y, \sigma_Y^2\}$. Via the additive properties of normal distributions, $logR$ is normally distributed with parameters $\mu_R = \mu_Y - \mu_X$ and $\sigma_R^2 = \sigma_X^2 + \sigma_Y^2 - 2\rho_{X,Y}\sigma_X\sigma_Y$. Thus, $R \sim Lognormal(\mu_R, \sigma_R^2)$, $E[R] = \exp\left(\mu_R + \frac{1}{2}\sigma_R^2\right)$, and $Var[R] = \exp(2\mu_R + 2\sigma_R^2) - \exp\left(2\mu_R + \sigma_R^2\right)$. This ratio can then be used to rescale a transposed rainstorm by selecting a random variate of R, denoted as r:

$$\tilde{x}_j = rx_i.$$

If X and Y are identically distributed then $E[R] = 1$, $Var[R] = 0$, and no rescaling is performed. If the distributions of X and Y are similar but not identical then $E[R]$ will be close to 1.0 and $Var[R]$ will be small. If the distributions are very different, then $E[R]$ may differ from 1.0 and $Var[R]$ may be relatively large.

Appendix B: Study-Specific Data and Software Usage

B.1 Rainfall Data

This study uses four rainfall datasets to perform various analyses:

NOAA Atlas 14: Rainfall IDF estimates from Volume 8 of NOAA's Atlas 14 project (Perica et al., 2013) were used for comparison purposes (i.e. Figure 2).

Stage IV: Stage IV (Lin, 2011) multisensor precipitation data from the National Oceanic and Atmospheric Administration (NOAA) was used for the SST analysis. Stage IV relies primarily on radar rainfall estimates from the NOAA National Weather Service (NWS) Next-Generation Radar Network (NEXRAD), bias adjusted using rain gage measurements. It has a resolution of roughly 20 km^2 and 60 minutes. Stage IV has been previously used in conjunction with SST and the RainyDay software (Wright et al., 2017; Yu et al., 2019; Zhu et al., 2018) as well as in many of evaluations of extreme rainfall and its impacts. The Stage IV dataset used in this analysis has been regridded from the HRAP projection to a regular latitude/longitude grid and converted into NetCDF files. This reformatted data is required for the RainyDay software and is available for download from this report's authors upon request.

PRISM Precipitation: Stage IV, like other radar-based datasets, suffers from "artifacts" caused by beam blockage, ground clutter, anomalous beam propagation, bright band contamination, and other radar-related issues (see Villarini and Krajewski, 2010). These artifacts were manually screened and, when clearly identifiable, removed when the RainyDay software was run. This is not feasible, however, for calculating the stochastic rescaling properties (see Appendix A2.3). Instead, we used daily, 0.04° precipitation provided by the Parameter-elevation Relationships on Independent Slopes Model (PRISM; (Daly et al., 2008, 1994) to estimate these rescaling properties.

INTENSE Subdaily Precipitation: Stage IV's roughly 20 km^2 spatial grid resolution is relatively coarse for simulating intense point-scale precipitation. Because of this, RainyDay has an optional feature to stochastically model the relationship between grid-scale and point-scale precipitation, when the latter estimates are desired. This is done by comparing co-located contemporaneous estimates of extreme precipitation accumulations from Stage IV and rain gage observations taken from the Global Subdaily Rainfall Dataset (Lewis et al., 2019). The ratios of the fifty largest co-located contemporaneous precipitation accumulations at both 6-hour and 24-hour durations were calculated over the domain shown in Figure 1. RainyDay allows the user to parameterize the empirical distributions of these ratios using either exponential or gamma distributions. These distributions, however, particularly for the 6-hour duration, were found to be overly variable. Instead, the mean values of these ratios were used. In other words, all RainyDay IDF values were multiplied by a constant factor to account for this point-area difference. This factor was 1.24 for the 6-hour duration and 1.16 for the 24-hour duration.

B.2 RainyDay Configuration

The following sections provide the specific configuration parameters used to populate the RainyDay input ".sst" files. All other required files are available upon request. Further explanation of the parameters can be found in the RainyDay user manual.

B.2.1 6-Hour Rainfall IDF Analysis ".sst" Configuration File Contents

```
MAINPATH	NRCS_project_2020
SCENARIONAME	RainyDay_Madison_6hr_updated_200km_STOCH_EXPON_DURCORR
RAINPATH	ST4.*.newregridded.nc
CATALOGNAME	StageIV_WI200km_Catalog_nolakes_updated.nc
CREATECATALOG	false
DURATION	6
DURATIONCORRECTION	true
NYEARS	1000
NREALIZATIONS	100
TIMESEPARATION	0
DOMAINTYPE	irregular
DOMAINSHP	WI200km_minusMIandLakes.shp
LATITUDE_MIN	42.25
LATITUDE_MAX	44.25
LONGITUDE_MIN	-91.0
LONGITUDE_MAX	-88.0
DIAGNOSTICPLOTS	false
FREQANALYSIS	true
SCENARIOS	false
SPINPERIOD	false
EXCLUDESTORMS
	8,13,29,33,40,41,68,86,120,123,125,143,144,161,166,183,201,239,245,256,276,284,285,288,291,297,319,
320,322,328,329,342,345,347,358,359,360
EXCLUDEMONTHS	1,2,3,12
TRANSPOSITION	nonuniform
RESAMPLING	poisson
RETURNLEVELS	2,5,10,25,50,100,200,500,1000
RETURNTHRESHOLD	1
UNCERTAINTY	90
RESCALING	stochastic
RAINDISTRIBUTIONFILE	PRISM_Top50storms_Daily_gridcell.nc
POINTAREA	point
POINTLAT	43.6
POINTLON	-90.9
```

B.2.2 24-Hour Rainfall IDF Analysis ".sst" Configuration File Contents

```
MAINPATH	NRCS_project_2020
SCENARIONAME	RainyDay_Madison_24hr_updated_200km_STOCH_GAMMA_DURCORR
RAINPATH	ST4.*.newregridded.nc
CATALOGNAME	StageIV_WI200km_Catalog_nolakes_updated.nc
CREATECATALOG	false
DURATION	24
DURATIONCORRECTION	true
NYEARS	1000
NREALIZATIONS	100
TIMESEPARATION	0
DOMAINTYPE	irregular
DOMAINSHP	WI200km_minusMIandLakes.shp
LATITUDE_MIN	42.25
LATITUDE_MAX	44.25
LONGITUDE_MIN	-91.0
LONGITUDE_MAX	-88.0
DIAGNOSTICPLOTS	false
```

```
FREQANALYSIS true
SCENARIOS	false
SPINPERIOD	false
EXCLUDESTORMS
	8,13,29,33,40,41,68,86,120,123,125,143,144,161,166,183,201,239,245,256,276,284,285,288,291,297,319,
320,322,328,329,342,345,347,358,359,360
EXCLUDEMONTHS	1,2,3,12
TRANSPOSITION	nonuniform
RESAMPLING	poisson
RETURNLEVELS2,5,10,25,50,100,200,500,1000
RETURNTHRESHOLD	1
UNCERTAINTY 90
RESCALING	stochastic
RAINDISTRIBUTIONFILE PRISM_Top50storms_Daily_gridcell.nc
POINTAREA	point
POINTLAT	43.6
POINTLON	-90.9
```

Appendix C: 6-Hour Duration Temporal Analysis

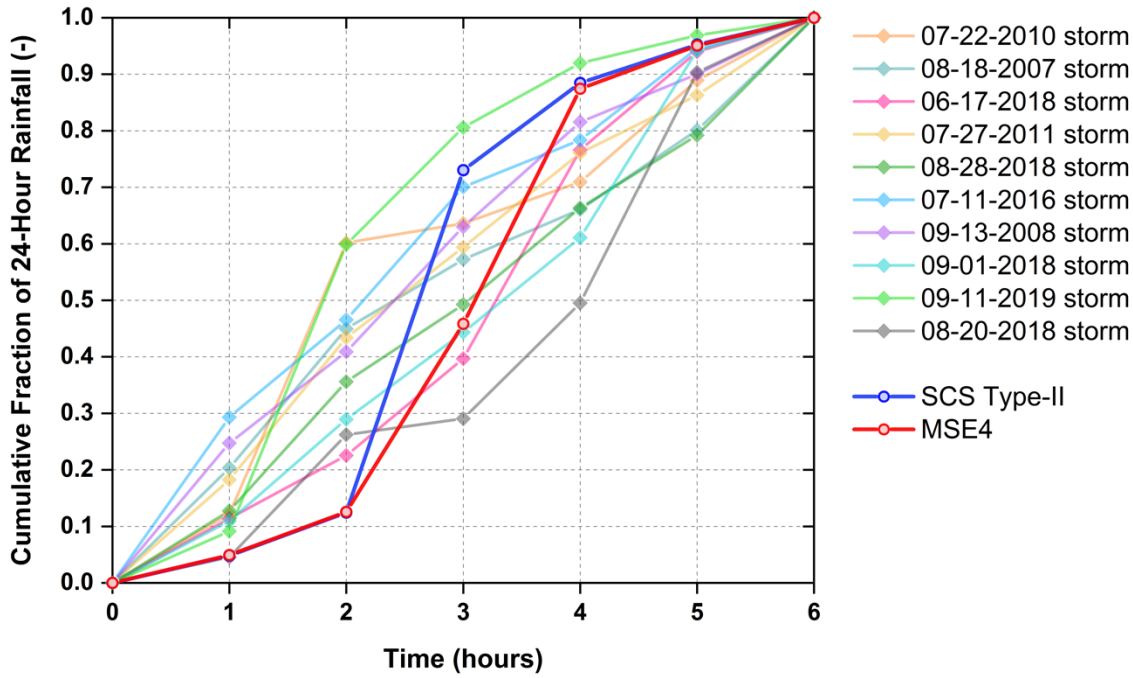

Figure C1: Same as Figure 3, but for the 6-hour duration.

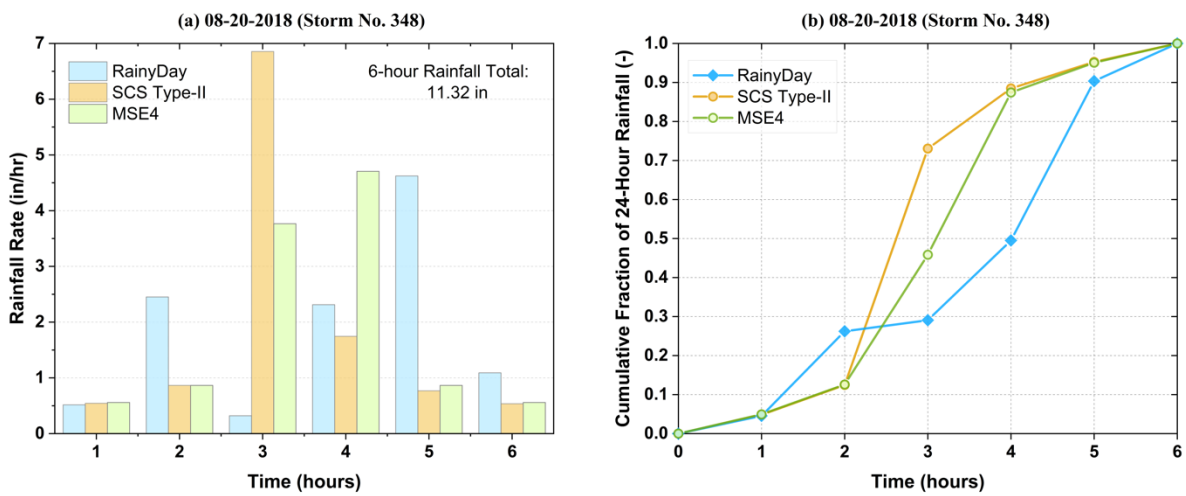

Figure C2: Same as Figure 4, but for the 6-hour duration.

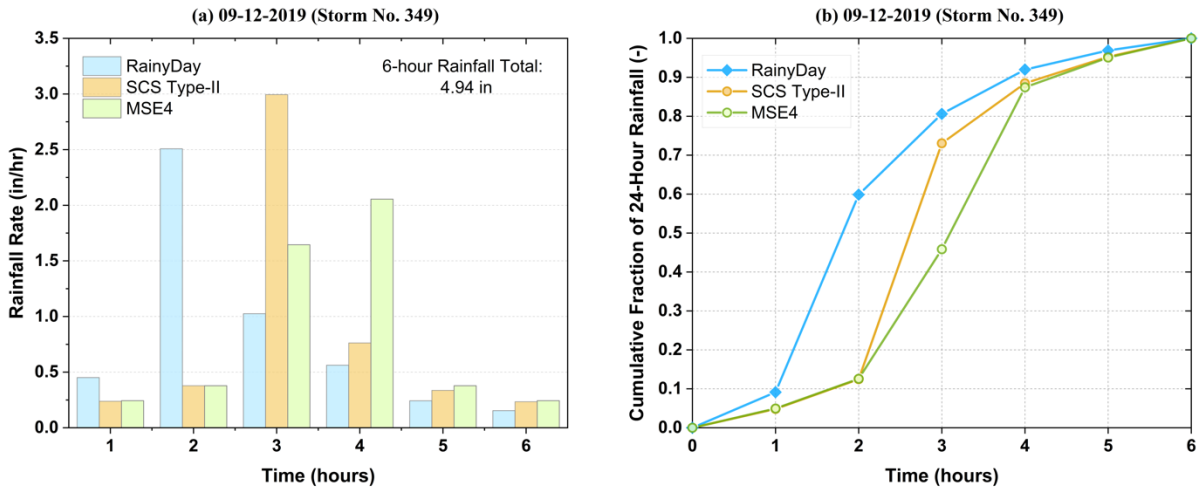

Figure C3: Same as Figure 5, but for the 6-hour duration.

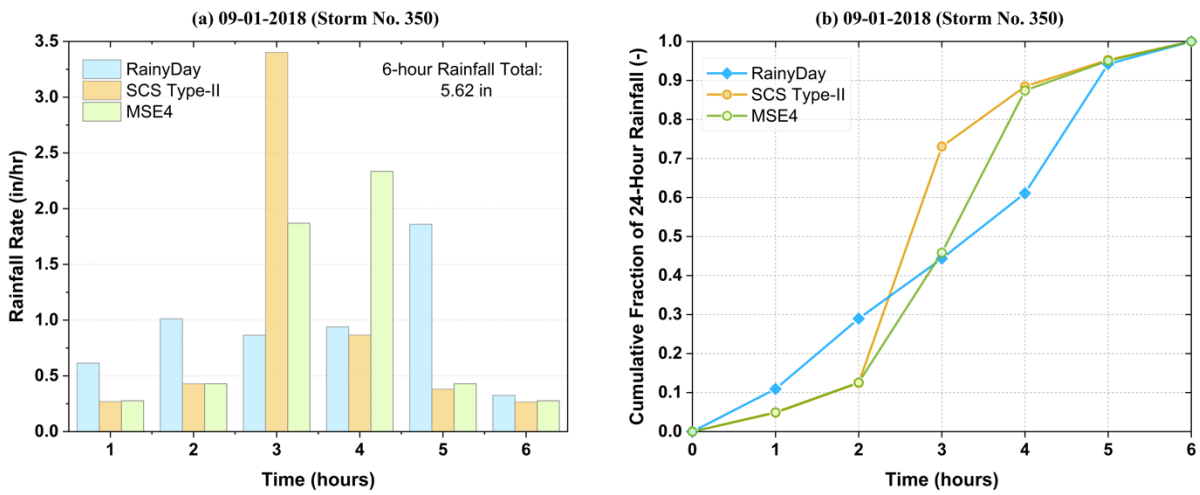

Figure C4: Same as Figure 6, but for the 6-hour duration.

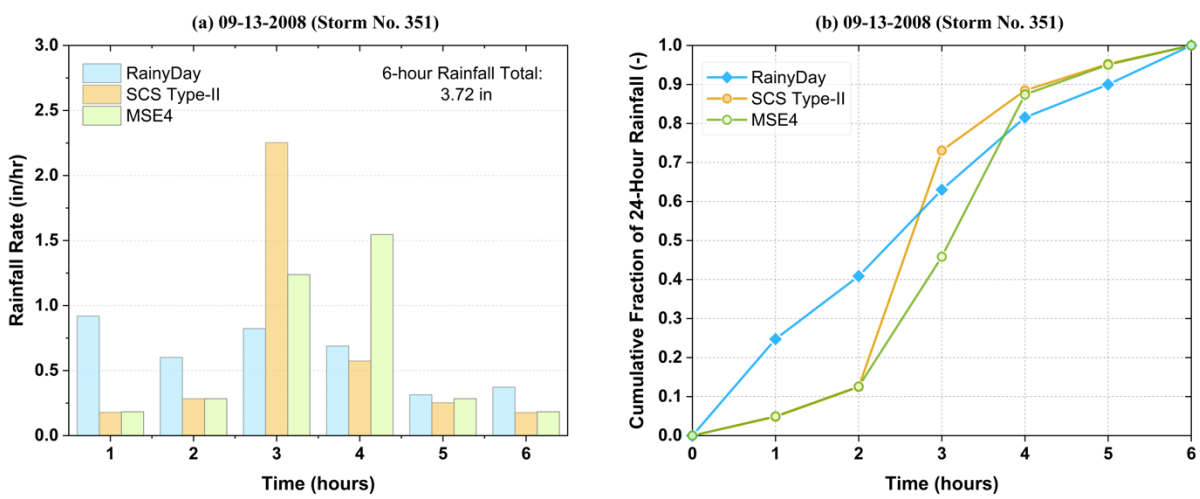

Figure C5: Same as Figure 7, but for the 6-hour duration.

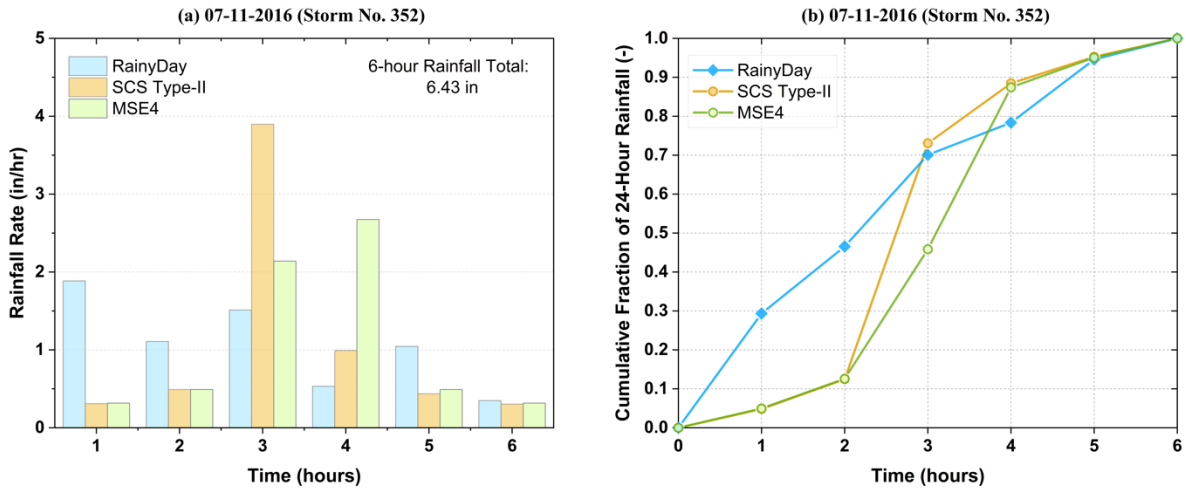

Figure C6: Same as Figure 8, but for the 6-hour duration.

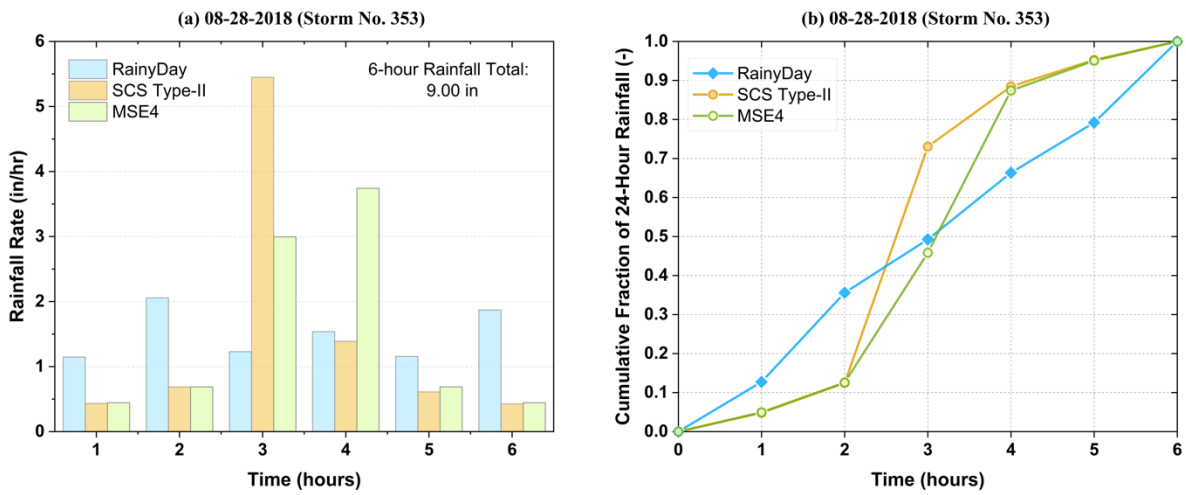

Figure C7: Same as Figure 9, but for the 6-hour duration.

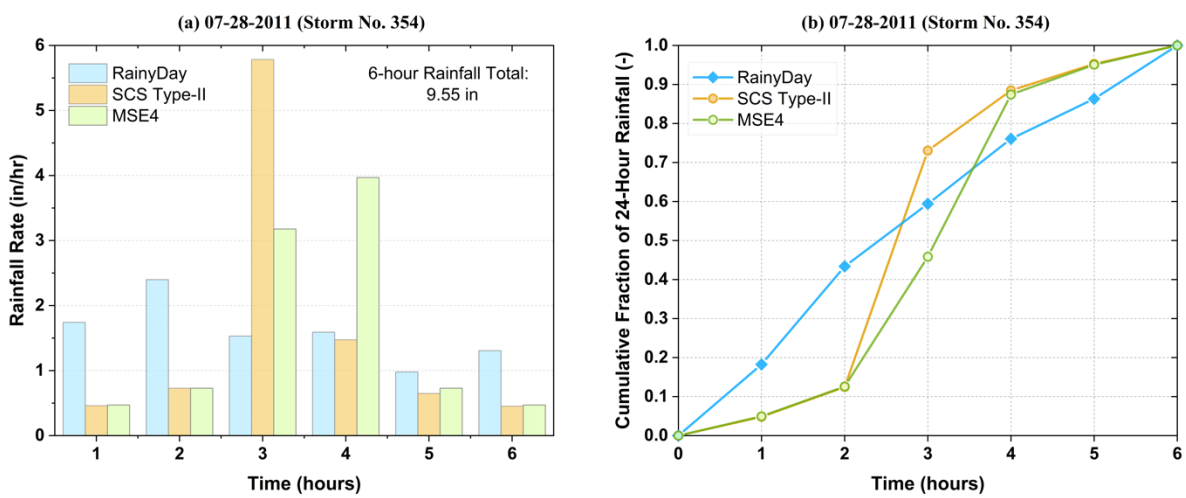

Figure C8: Same as Figure 10, but for the 6-hour duration.

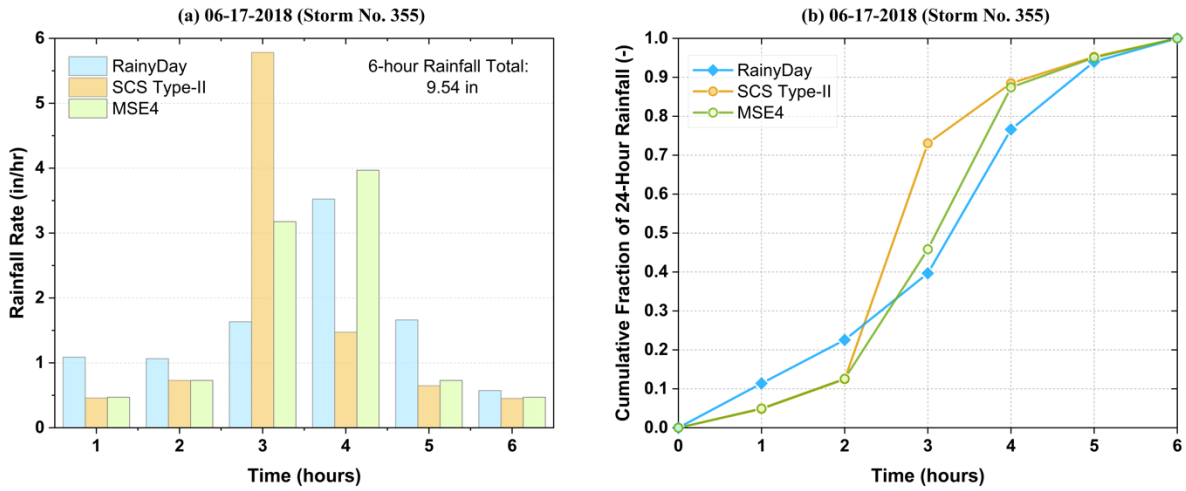

Figure C9: Same as Figure 11, but for the 6-hour duration.

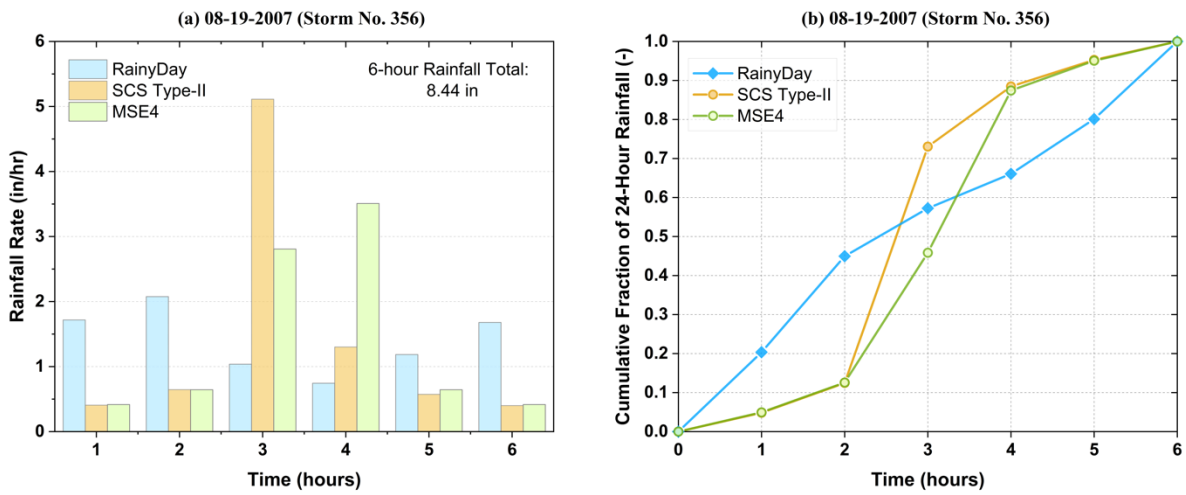

Figure C10: Same as Figure 12, but for the 6-hour duration.

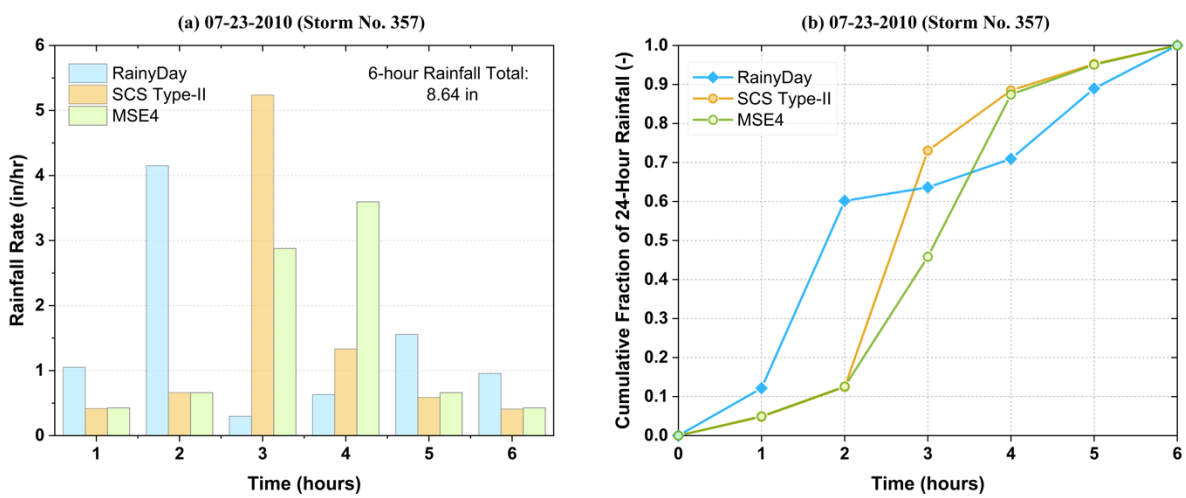

Figure C11: Same as Figure 13, but for the 6-hour duration.

Appendix D: 28 August 2018 Hyetographs

The accompanying Excel file "NRCS_Aug-28-2018_Hyetographs.xlsx" contains the observed maximum 6-hour and 24-hour hyetographs for the 28 August 2018 storm, as well as corresponding SCS/NRCS Type-II and MSE4 design storms. In addition, 72-hour hyetographs for the approximate centers of the Coon Creek and West Fork Kickapoo watersheds are provided.

Note that these observed hyetographs on worksheets "6-hr Hyetographs" and "24-hr Hyetographs" are not suitable for calibration for a specific watershed, since they are derived from the location of maximum rainfall, rather than a specific watershed. Rather, calibration should be performed using the 72-hour hyetographs found in the worksheets "Hyetograph_WForkKickapoo" and "Hyetograph_CoonCreek".

All hyetographs are at the hourly scale, based on the Stage IV combined radar and rain gage dataset (see Appendix B). This dataset can have inaccuracies, and whether or not hourly resolution rainfall data are sufficient for hydrologic modeling of this flood event and these watersheds is beyond the scope of this study.